

# Secrecy Analysis of Energy-Harvesting Backscatter Communications with Tag Selection in Nakagami- $m$ Fading

Mohammad Nafees, *Student Member, IEEE*, Dharmendra Dixit, *Member, IEEE*,  
and Arvind Kumar, *Member, IEEE*

## Abstract

Backscatter communication is an energy-efficient technique that enables sustainable wireless connectivity with a minimal environmental impact. In this paper, the secrecy performance of practical non-linear energy-harvesting backscatter communications with various tag selection schemes is analyzed in Nakagami- $m$  fading channels. We consider four tag selection schemes: sub-optimal, minimal eavesdropping, optimal, and random tag selection. Closed-form expressions for secrecy outage probability (SOP) and intercept probability (IP) are derived for each scheme, along with asymptotic expressions to provide deeper insights. The impact of system and fading parameters on SOP and IP is investigated, and simulation results are presented to validate the accuracy of the analytical expressions.

## Index Terms

Energy-harvesting, backscatter communications, tag selection, secrecy outage probability, intercept probability.

## I. INTRODUCTION

As multi-device internet-of-things (IoT) ecosystems continue to expand, future wireless technologies such as sixth-generation (6G) networks face significant challenges in spectrum optimization and power consumption, particularly in low-cost, low-power, and battery-free systems [1]–[3]. Backscatter communication (BackCom) is an emerging technology that addresses these

The authors are with the Electronics and Communication Engineering Department, Motilal Nehru National Institute of Technology Allahabad, Prayagraj, 211004, India e-mail: (nafeesiiit@gmail.com (arvindk, dharmendradixit))@mnnit.ac.in

challenges by enabling devices to transmit information through the modulation of ambient radio signals without requiring dedicated power sources. This innovative method has garnered significant attention in IoT applications due to its minimal power requirements and potential for widespread deployment. However, BackCom's relatively simple transmission structure makes it vulnerable to passive eavesdropping, where adversaries may intercept and decode transmitted data. Furthermore, the shared nature of the unlicensed wireless spectrum introduces concerns regarding interference and unauthorized access. Therefore, securing BackCom systems is essential. Physical layer security (PLS) is a promising solution to ensure secure communication between authorized nodes with minimal complexity and high efficiency [3]–[5]. By leveraging physical characteristics like noise and channel fluctuations, PLS enhances security, making it a promising approach for safeguarding BackCom systems.

#### A. Related Works

Several studies in the literature have investigated the secrecy performance of BackCom systems. In [6], the secrecy outage probability (SOP) for a passive BackCom system with multiple tags is derived for Rayleigh fading channels. The secrecy rate (SR) of a single-reader, single-tag model is analyzed across various scenarios using analytical methods in [7]. In [8], the authors obtained the exact and asymptotic SOP expressions for a multi-tag BackCom system in correlated Rayleigh fading channels. In [9], analytical expressions for ergodic secrecy capacity (ESC) and SOP are derived for a multi-tag self-powered BackCom network using a proposed tag selection strategy in Nakagami- $m$  fading. In [10] the exact and asymptotic SOPs are presented for multi-tag ambient BackCom systems, considering motion and imperfect channel estimation in Rayleigh fading. In [11], the bit error rate performance of ambient BackCom systems in Rayleigh fading was investigated through theoretical and simulation results. In [12], expressions for the SOP and intercept probability (IP) of a multi-tag BackCom network with a practical non-linear energy-harvesting (EH) model are derived in Rayleigh fading for four tag selection schemes: sub-optimal tag selection (SOTS), minimal eavesdropping tag selection (METS), optimal tag selection (OTS), and random tag selection (RTS). Based on this literature survey and to the best of the author's knowledge, the secrecy performance of BackCom systems incorporating practical non-linear EH models and tag selection schemes (SOTS, METS, OTS, RTS) has not been explored in the context of versatile Nakagami- $m$  fading model.

## B. Motivation and Contributions

Nakagami- $m$  fading distribution is widely used to model various wireless propagation scenarios, such as urban and indoor environments, due to its flexibility in characterizing different fading conditions [13]. This adaptability makes it crucial for designing robust BackCom systems, ensuring enhanced performance and reliability. Despite the practical significance of Nakagami- $m$  fading, the secrecy performance of BackCom systems with practical non-linear EH models and tag selection schemes remains unexplored. In this work, we investigate the secrecy performance of a multi-tag BackCom network under Nakagami- $m$  fading for four tag selection protocols: SOTS, METS, OTS, and RTS.

The key contributions of this work can be summarized as follows:

- i) We derive new closed-form analytical expressions for SOP and IP for each selection scheme in Nakagami- $m$  fading channels.
- ii) To provide deeper insights, we also derive asymptotic expressions for SOP and IP for each selection scheme.
- iii) We examine the impact of variations in the number of tags, distances, and threshold rates on the performance of the BackCom system.
- iv) Notably, our generalized analytical expressions include the existing results for Rayleigh fading channels as a special case when  $m = 1$ .

The structure of the paper is as follows: Section II introduces the system and channel models. Section III details the performance evaluation for the considered system under various tag selection protocols. Numerical results and their analysis are provided in Section IV. Finally, the conclusions are summarized in Section V.

## II. SYSTEM AND CHANNEL MODEL

In this study, we consider a BackCom system as shown in Fig. 1. It has a source node  $S$ ,  $N$  tags  $\mathcal{T}_k$  that have energy harvesting units, where  $k \in \{1, 2, \dots, N\}$ , a destination node  $D$ , and an eavesdropper node  $E$ . Each node in the system is assumed to operate with a single antenna configuration. Each tag contains distinct information that needs to be conveyed to  $D$ , ensuring each tag's data is unique. Therefore,  $S$  selects a single tag per transmission to relay its specific information. Let  $\mathcal{X} \in \{D, E\}$ , with the link between  $S$  and  $\mathcal{T}_k$  denoted as  $S - \mathcal{T}_k$  and the link between  $\mathcal{T}_k$  and  $\mathcal{X}$  represented as  $\mathcal{T}_k - \mathcal{X}$ . The complex channel coefficient for  $S - \mathcal{T}_k$  link can be expressed as  $h_{sk} = \sqrt{d_{sk}'^{-\alpha_{sk}}} g_{sk} e^{-j\tilde{\Theta}_{sk}}$ , where  $d_{sk}'$ ,  $\alpha_{sk}$ ,  $g_{sk}$  and  $\tilde{\Theta}_{sk}$  corresponds to the

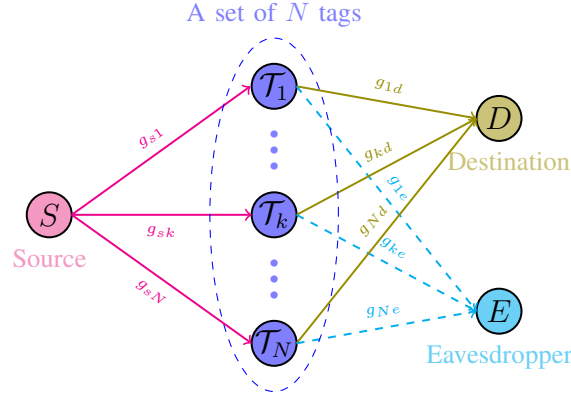


Fig. 1. System model illustrating energy-harvesting backscatter communications with multiple tags, a single destination, and an eavesdropper

distance, path loss exponent, fading gain and phase, respectively. Similarly, the  $\mathcal{T}_k - \mathcal{X}$  link's channel coefficient can be expressed as  $h_{kx} = \sqrt{d'_{kx}{}^{-u_{kx}}} g_{kx} e^{-j\tilde{\Theta}_{kx}}$ , with  $d'_{kx}$ ,  $u_{kx}$ ,  $g_{kx}$  and  $\tilde{\Theta}_{kx}$  representing the distance, path loss exponent, fading gain, and phase. We assume that the channel gains  $g_{sk}$  and  $g_{kx}$  for each  $k$  are independent but non-identically distributed (i.n.i.d.), following a Nakagami- $m$  fading model. The phases  $\tilde{\Theta}_{sk}$  and  $\tilde{\Theta}_{kx}$  are independently uniformly distributed over the interval  $-\pi$  to  $\pi$ . The probability density function (PDF) for each  $g_{sk}^2$  and  $g_{kx}^2$  can be given as follows [14, (2)]:

$$f_{g_{sk}^2}(t) = \frac{\tilde{\lambda}_{sk}^{m_{sk}} t^{m_{sk}-1}}{\Gamma(m_{sk})} \exp(-\tilde{\lambda}_{sk} t), \quad (1)$$

$$f_{g_{kx}^2}(t) = \frac{\tilde{\lambda}_{kx}^{m_{kx}} t^{m_{kx}-1}}{\Gamma(m_{kx})} \exp(-\tilde{\lambda}_{kx} t), \quad (2)$$

where  $\Gamma(\cdot)$  denotes the gamma function,  $\tilde{\lambda}_{sk} = m_{sk}/\Omega_{sk}$ ,  $\tilde{\lambda}_{kx} = m_{kx}/\Omega_{kx}$ ,  $\Omega_{sk}$  and  $\Omega_{kx}$  represent average value of  $g_{sk}^2$  and  $g_{kx}^2$ , respectively, and  $m_{sk}$  and  $m_{kx}$  represent fading parameter for  $g_{sk}^2$  and  $g_{kx}^2$ , respectively [13]. By applying the formulas [15, (8.351.2),(8.352.1)] into [14, (3)], the corresponding cumulative distribution function (CDF) expression for each  $g_{sk}^2$  and  $g_{kx}^2$  can be given as

$$F_{g_{sk}^2}(t) = \mathbb{P}(g_{sk}^2 < t) = \frac{\gamma(m_{sk}, \tilde{\lambda}_{sk} t)}{\Gamma(m_{sk})} = 1 - \sum_{j=0}^{m_{sk}-1} \frac{\exp(-\tilde{\lambda}_{sk} t)}{(\tilde{\lambda}_{sk} t)^{-j} \Gamma(j+1)}, \quad (3)$$

and

$$F_{g_{kx}^2}(t) = \mathbb{P}(g_{kx}^2 < t) = \frac{\gamma(m_{kx}, \tilde{\lambda}_{kx}t)}{\Gamma(m_{kx})} = 1 - \sum_{j=0}^{m_{kx}-1} \frac{\exp(-\tilde{\lambda}_{kx}t)}{(\tilde{\lambda}_{kx}t)^{-j} \Gamma(j+1)}, \quad (4)$$

respectively, where  $\mathbb{P}[\cdot]$  refers to the probability of an event occurring and  $\gamma(\cdot, \cdot)$  is the lower incomplete gamma function [15, 8.350.1].

Let  $m_s$  represent the unit energy message symbol sent by the source node  $S$ , and the received signal at  $\mathcal{T}_k$  is then given by

$$y_k = \sqrt{\mathcal{P}} h_{sk} m_s, \quad (5)$$

where  $\mathcal{P}$  is the transmission power of  $S$ . The noise in the received signal at  $\mathcal{T}_k$  is assumed negligible, as it is substantially lower than the RF signal strength [16]. The signal received at  $\mathcal{T}_k$  is further partition into two parts:  $\sqrt{1 - \delta_n} y_k(t)$  for EH and  $\sqrt{\delta_n} y_k(t)$  for BackCom, where  $\delta_n$  represents the dynamic optimal reflection coefficient of  $\mathcal{T}_k$ . The input power for the energy harvesting unit at  $\mathcal{T}_k$  is given by  $\mathcal{P}_k^i = (1 - \delta_k) \mathcal{P} d_{sk}'^{-u_{sk}} g_{sk}^2$ . For the non-linear EH model, the harvested power at  $\mathcal{T}_k$  is represented as [17]

$$\mathcal{P}_k^o = \frac{\mathcal{P}_{\mathcal{T}_k}^{max} (1 - \exp(-\xi_1 \mathcal{P}_k^i + \xi_1 \xi_0))}{1 + \exp(-\xi_1 \mathcal{P}_k^i + \xi_1 \xi_2)}, \quad (6)$$

where  $\mathcal{P}_{\mathcal{T}_k}^{max}$  indicates the saturation power level when  $\mathcal{P}_k^i$  is considerably high and  $\xi_0$ ,  $\xi_1$ , and  $\xi_2$  represent the sensitivity threshold, resistance, capacitance, respectively.  $\mathcal{P}_{\mathcal{T}_k}^c$  refers to the power consumed by the tag's circuit. Due to the energy causality,  $k$ -th tag  $\mathcal{T}_k$  can only reflect the source's signal to  $D$  if  $\mathcal{P}_k^o \geq \mathcal{P}_{\mathcal{T}_k}^c$ . Consequently, to optimize the power of the backscatter signal,  $\mathcal{P}_k^o = \mathcal{P}_{\mathcal{T}_k}^c$  must be satisfied. Considering  $0 \leq \beta_k^* \leq 1$ , the optimal dynamic reflection coefficient [17] can be formulated as

$$\beta_k^* = \max\left(1 - \frac{\phi}{\mathcal{P} d_{sk}'^{-u_{sk}} g_{sk}^2}, 0\right), \quad (7)$$

where  $\phi = \xi_1^{-1} \ln(\phi_1/\phi_2)$ ,  $\phi_1 = \mathcal{P}_{\mathcal{T}_k}^{max} \exp(\xi_1 \xi_2) + \mathcal{P}_{\mathcal{T}_k}^c \exp(\xi_1 \xi_0)$ ,  $\phi_2 = \mathcal{P}_{\mathcal{T}_k}^{max} - \mathcal{P}_{\mathcal{T}_k}^c$ .  $\beta_k^*$  in As seen from (7), when  $\beta_k^* > 0$ ,  $\mathcal{T}_k$  has sufficient energy to reflect the signal, however, if  $\beta_k^* = 0$ ,  $\mathcal{T}_k$  is unable to perform the reflection. Using (5) and (7), the backscatter signal at  $\mathcal{T}_k$  is given

by

$$\hat{y}_k = \sqrt{\zeta\beta_k^*}y_k c_k = \sqrt{\zeta\beta_k^* \mathcal{P}}h_{sk}m_s c_k \quad (8)$$

where  $c_k$  is the transmitted signal from  $\mathcal{T}_k$  with unit energy, and  $\zeta$  is the tag scattering coefficient [16]. The signal received at  $\mathcal{X}$  can be formulated as

$$y_x = \sqrt{\zeta\beta_k^* \mathcal{P}}h_{sk}h_{kx}m_s c_k + w_x, \quad (9)$$

where  $w_x$  is the additive white Gaussian noise (AWGN) at  $\mathcal{X}$ , having a zero mean and a variance of  $\sigma^2$ . Thus, the instantaneous signal-to-noise ratio (SNR) at  $\mathcal{X}$  can be given as

$$\gamma_x^k = \zeta\beta_k^* d_{sk}^{\prime -u_{sk}} d_{kx}^{\prime -u_{kx}} g_{sk}^2 g_{kx}^2 \frac{\Gamma_t}{\Gamma_p}, \quad (10)$$

where  $\Gamma_t = \frac{\mathcal{P}}{\sigma^2}$  represents the average transmit SNR and  $\Gamma_p$  denotes the performance gap due to the applied modulation scheme.

### III. PERFORMANCE ANALYSIS WITH TAG SELECTION

This section provides both exact and asymptotic analyses of SOP and IP for various tag selection protocols.

#### A. Exact SOP Analysis

The SOP of the considered BackCom system model is defined as the probability that the secrecy rate  $\mathcal{C}_{sec}(\gamma_d^k, \gamma_e^k)$  falls below a specified threshold rate  $\mathcal{R}$ , i.e. [12]

$$\tilde{P}(\mathcal{R}) = \mathbb{P}[\mathcal{C}_{sec}(\gamma_d^k, \gamma_e^k) < \mathcal{R}], \quad (11)$$

where  $\mathcal{C}_{sec}(\gamma_d^k, \gamma_e^k)$  is expressed as [12, (8)]

$$\mathcal{C}_{sec}(\gamma_d^k, \gamma_e^k) = \max\left(\log_2\left(\frac{1 + \gamma_d^k}{1 + \gamma_e^k}\right), 0\right). \quad (12)$$

The SOP for the  $k$ -th tag can be categorized into two cases for each selection scheme: Case 1, where the harvested power at  $\mathcal{T}_k$  is insufficient to power its circuit, indicated by  $\beta_k^* = 0$ ; Case 2, where the harvested power meets  $\mathcal{T}_k$ 's minimum power requirements, but the resulting secrecy capacity is below the threshold  $\mathcal{R}$ , represented by  $\beta_k^* > 0$  and  $\mathcal{C}_{sec}(\gamma_d^k, \gamma_e^k) < \mathcal{R}$ .

1) *SOTS Protocol*: In the SOTS protocol, the tag selected for communication is the one with the highest power gain among all  $h_{kd}$  links, defined as:

$$k^* = \arg \max_{1 \leq k \leq N} \{g_{kd}^2\}. \quad (13)$$

Here, since  $g_{kd}^2$  variables are independent and identically distributed (i.i.d.), the CDF of  $g_{k^*d}^2$  can be written using order statistics as [14, (4)]

$$F_{g_{k^*d}^2}(t) = \left(F_{g_{kd}^2}(t)\right)^N. \quad (14)$$

Using (4) into (14) and simplifying the result using multinomial theorem [18, (24.1.2.B)], the CDF of  $g_{k^*d}^2$  is expressed as

$$\begin{aligned} F_{g_{k^*d}^2}(t) &= \left(1 - \sum_{j=0}^{m_{kd}-1} \frac{\exp(-\tilde{\lambda}_{kd}t)}{(\tilde{\lambda}_{kd}t)^{-j} \Gamma(j+1)}\right)^N \\ &= \sum_{\substack{n_1, n_2, \dots, n_{m_{kd}+1} \geq 0 \\ n_1 + n_2 + \dots + n_{m_{kd}+1} = N}} \delta(N, \theta_1, \theta_2, \tilde{\lambda}_{kd}) t^{\theta_2} \exp(-\tilde{\lambda}_{kd}\theta_1 t), \end{aligned} \quad (15)$$

where  $\theta_1 = n_2 + n_3 + \dots + n_{m_{kd}+1}$ ,  $\theta_2 = n_3 + 2n_4 + \dots + (m_{kd} - 1)n_{m_{kd}+1}$ , and

$$\delta(N, \theta_1, \theta_2, \tilde{\lambda}_{kd}) = \frac{(-1)^{\theta_1} \tilde{\lambda}_{kd}^{\theta_2} \Gamma(N+1)}{\left(\prod_{i=1}^{m_{kd}+1} \Gamma(n_i+1)\right) \left(\prod_{i=1}^{m_{kd}} (\Gamma(i))^{n_{i+1}}\right)}.$$

Applying results from (11) and (13), the SOP for the SOTS protocol is formulated as [12]

$$\tilde{P}_{out} = \underbrace{\mathbb{P}(\beta_k^* = 0)}_{=\tilde{P}_1} + \underbrace{\mathbb{P}(\beta_k^* > 0, \mathcal{C}_{sec}(\gamma_d^{k^*}, \gamma_e^k) < \mathcal{R})}_{=\tilde{P}_2}. \quad (16)$$

Using (3) and (7),  $\tilde{P}_1$  can be represented as

$$\begin{aligned} \tilde{P}_1 &= \mathbb{P}\left(\max\left(1 - \frac{\phi}{\mathcal{P}d_{sk}'^{-u_{sk}} |g_{sk}|^2}, 0\right) = 0\right) = \mathbb{P}\left(g_{sk}^2 < \frac{\phi}{\mathcal{P}d_{sk}'^{-u_{sk}}}\right) \\ &= F_{g_{sk}^2}\left(\frac{\phi}{\mathcal{P}d_{sk}'^{-u_{sk}}}\right) = \frac{\gamma\left(m_{sk}, \frac{\tilde{\lambda}_{sk}\phi}{\mathcal{P}d_{sk}'^{-u_{sk}}}\right)}{\Gamma(m_{sk})}. \end{aligned} \quad (17)$$

Using (7) and (12),  $\tilde{P}_2$  can be represented as

$$\tilde{P}_2 = \mathbb{P}(\beta_k^* > 0, \mathcal{C}_{sec}(\gamma_d^{k^*}, \gamma_e^k) < \mathcal{R}) = \mathbb{P}\left(g_{sk}^2 < \frac{\phi}{\mathcal{P}d_{sk}^{\prime -u_{sk}}}, \frac{1 + \beta_k^* \Gamma_t \eta_1 g_{sk}^2 g_{k^*d}^2}{1 + \beta_k^* \Gamma_t \eta_2 g_{sk}^2 g_{ke}^2} < \tau\right), \quad (18)$$

where  $\tau = 2^{\mathcal{R}}$ ,  $\eta_1 = \frac{\zeta d_{sk}^{\prime -u_{sk}} d_{kd}^{\prime -u_{kd}}}{\Gamma_p}$ , and  $\eta_2 = \frac{\zeta d_{sk}^{\prime -u_{sk}} d_{ke}^{\prime -u_{ke}}}{\Gamma_p}$ . In deriving  $\tilde{P}_2$ , the transformations of the random variables  $W_1 = g_{sk}^2$ ,  $W_2 = g_{k^*d}^2$ , and  $W_3 = g_{ke}^2$  are considered. We can reformulate  $\tilde{P}_2$  as

$$\begin{aligned} \tilde{P}_2 &= \mathbb{P}\left(W_1 > \frac{\phi}{\mathcal{P}d_{sk}^{\prime -u_{sk}}}, W_2 < \frac{\tau - 1}{\beta_k^* \eta_1 \Gamma_t w_1} + \frac{\tau \eta_2 w_3}{\eta_1}\right) \\ &= \int_0^\infty \int_{\frac{\phi}{\mathcal{P}d_{sk}^{\prime -u_{sk}}}}^\infty F_{W_2}\left(\frac{\tau - 1}{\beta_k^* \eta_1 \Gamma_t w_1} + \frac{\tau \eta_2 w_3}{\eta_1}\right) f_{W_1}(w_1) f_{W_3}(w_3) dw_1 dw_3. \end{aligned} \quad (19)$$

By substituting  $F_{W_2}(\cdot)$ ,  $f_{W_1}(\cdot)$  and  $f_{W_3}(\cdot)$  into (19) and evaluating the resulting integrals, a closed-form expression for  $\tilde{P}_2$  can be obtained, as

$$\begin{aligned} \tilde{P}_2 &= \left(\frac{\tilde{\lambda}_{sk}^{m_{sk}} \tilde{\lambda}_{ke}^{m_{ke}}}{\Gamma(m_{sk}) \Gamma(m_{ke})}\right) \sum_{\substack{n_1, n_2, \dots, \\ n_{m_{kd}+1} \geq 0 \\ n_1 + n_2 + \dots + n_{m_{kd}+1} = N}} \delta(N, \theta_1, \theta_2, \tilde{\lambda}_{kd}) \sum_{q=0}^{\theta_2} \binom{\theta_2}{q} \left(\frac{\tau \eta_2}{\eta_1}\right)^q \exp\left(-\frac{\tilde{\lambda}_{sk} \phi}{\mathcal{P}d_{sk}^{\prime -u_{sk}}}\right) \\ &\quad \times \left(\frac{\tau - 1}{\eta_1 \Gamma_t}\right)^{\theta_2 - q} \sum_{p=0}^{m_{sk} - 1} \binom{m_{sk} - 1}{p} \left(\frac{\phi}{\mathcal{P}d_{sk}^{\prime -u_{sk}}}\right)^{m_{sk} - 1 - p} 2 \left(\frac{\tilde{\lambda}_{kd} \theta_1 (\tau - 1)}{\eta_1 \Gamma_t \tilde{\lambda}_{sk}}\right)^{\frac{p + q - \theta_2 + 1}{2}} \\ &\quad \times K_{p+q-\theta_2+1} \left(\sqrt{\frac{4\theta_1 \tilde{\lambda}_{sk} \tilde{\lambda}_{kd} (\tau - 1)}{\eta_1 \Gamma_t}}\right) \left(\tilde{\lambda}_{ke} + \frac{\tilde{\lambda}_{kd} \theta_1 \tau \eta_2}{\eta_1}\right)^{-m_{ke} - q} \Gamma(m_{ke} + q), \end{aligned} \quad (20)$$

where  $K_u(\cdot)$  represents the modified Bessel function of the second kind of  $u$ -th order [15]. A detail solution of  $\tilde{P}_2$  for the SOTS protocol is given in Appendix A. The exact SOP for the SOTS protocol is provided in Table I on page 12.

2) *METS Protocol*: In this protocol, the tag is chosen based on identifying the weakest  $\mathcal{T}_k - E$  link. This selection method for minimizing eavesdropping can be represented as

$$k^* = \arg \min_{1 \leq k \leq N} \{g_{ke}^2\} \quad (21)$$



Here, since  $g_{ke}^2$  variables are i.i.d., the CDF of  $g_{k^*e}^2$  can be written using binomial expansion as

$$\begin{aligned} F_{g_{k^*e}^2}(t) &= 1 - (1 - \mathbb{P}(g_{ke}^2 < t))^N = 1 - (1 - F_{g_{ke}^2}(t))^N \\ &= \sum_{l=1}^N \binom{N}{l} (-1)^{l+1} (F_{g_{ke}^2}(t))^l \end{aligned} \quad (22)$$

Using (4) into (22) and simplifying the result using multinomial theorem [18, (24.1.2.B)], the CDF of  $g_{k^*e}^2$  is expressed as

$$\begin{aligned} F_{g_{k^*e}^2}(t) &= \sum_{l=1}^N \binom{N}{l} (-1)^{l+1} \left( 1 - \sum_{j=0}^{m_{ke}-1} \frac{\exp(-\tilde{\lambda}_{kd}t)}{(\tilde{\lambda}_{ke}t)^{-j} \Gamma(j+1)} \right)^l \\ &= \sum_{l=1}^N \binom{N}{l} (-1)^{l+1} \sum_{\substack{n_1, n_2, \dots, n_{m_{ke}+1} \geq 0 \\ n_1 + n_2 + \dots + n_{m_{ke}+1} = l}} \delta_2(l, \theta_3, \theta_4, \tilde{\lambda}_{ke}) t^{\theta_4} \exp(-\tilde{\lambda}_{ke}\theta_3 t). \end{aligned} \quad (23)$$

where  $\theta_3 = n_2 + n_3 + \dots + n_{m_{ke}+1}$ ,  $\theta_4 = n_3 + 2n_4 + \dots + (m_{ke} - 1)n_{m_{ke}+1}$ , and

$$\delta_2(l, \theta_3, \theta_4, \tilde{\lambda}_{ke}) = \frac{(-1)^{\theta_3} \tilde{\lambda}_{ke}^{\theta_4} \Gamma(l+1)}{(\prod_{i=1}^{m_{ke}+1} \Gamma(n_i + 1)) (\prod_{i=1}^{m_{ke}} (\Gamma(i))^{n_{i+1}})}.$$

The PDF of  $g_{k^*e}^2$  can be obtained by differentiating  $F_{g_{k^*e}^2}(t)$  with respect to  $t$  which is given in (24) on page 5.

$$\begin{aligned} f_{g_{k^*e}^2}(t) &= \sum_{l=1}^N \binom{N}{l} (-1)^{l+1} \sum_{\substack{n_1, n_2, \dots, n_{m_{ke}+1} \geq 0 \\ n_1 + n_2 + \dots + n_{m_{ke}+1} = l}} \delta_2(l, \theta_3, \theta_4, \tilde{\lambda}_{ke}) \\ &\quad \times \left( \theta_4 t^{\theta_4-1} \exp(-\tilde{\lambda}_{ke}\theta_3 t) - \tilde{\lambda}_{ke}\theta_3 t^{\theta_4} \exp(-\tilde{\lambda}_{ke}\theta_3 t) \right). \end{aligned} \quad (24)$$

Applying results from (11) and (21), the SOP for the METS protocol is formulated as [12]

$$\tilde{P}_{out} = \underbrace{\mathbb{P}(\beta_k^* = 0)}_{=\tilde{P}_1} + \underbrace{\mathbb{P}(\beta_k^* > 0, \mathcal{C}_{sec}(\gamma_d^k, \gamma_e^{k^*}) < \mathcal{R})}_{=\tilde{P}_2}. \quad (25)$$

Using a method akin to the SOTS, the expression for  $\tilde{P}_1$  is provided in (17). Using (11) and (21),  $\tilde{P}_2$  can be formulated as

$$\tilde{P}_2 = \mathbb{P}(\beta_k^* > 0, \mathcal{C}_{sec}(\gamma_d^k, \gamma_e^k) < \mathcal{R}) = \mathbb{P}\left(g_{sk}^2 < \frac{\phi}{\mathcal{P}d_{sk}'^{-u_{sk}}}, \frac{1 + \beta_k^* \Gamma_t \eta_1 g_{sk}^2 g_{kd}^2}{1 + \beta_k^* \Gamma_t \eta_2 g_{sk}^2 g_{k^*e}^2} < \tau\right). \quad (26)$$

In deriving  $\tilde{P}_2$ , the transformations of the random variables  $W_1 = g_{sk}^2$ ,  $W_2 = g_{k^*d}^2$ , and  $W_3 = g_{ke}^2$  are considered. We can reformulate  $\tilde{P}_2$  as

$$\begin{aligned}\tilde{P}_2 &= \mathbb{P}\left(W_1 > \frac{\phi}{\mathcal{P}d_{sk}'^{-u_{sk}}}, W_2 < \frac{\tau - 1}{\beta_n^* \eta_1 \Gamma_t w_1} + \frac{\tau \eta_2 w_3}{\eta_1}\right) \\ &= \int_0^\infty \int_{\frac{\phi}{\mathcal{P}d_{sk}'^{-u_{sk}}}}^\infty F_{W_2}\left(\frac{\tau - 1}{\beta_n^* \eta_1 \Gamma_t w_1} + \frac{\tau \eta_2 w_3}{\eta_1}\right) f_{W_1}(w_1) f_{W_3}(w_3) dw_1 dw_3.\end{aligned}\quad (27)$$

By substituting  $F_{W_2}(\cdot)$ ,  $f_{W_1}(\cdot)$  and  $f_{W_3}(\cdot)$  into (27) and evaluating the resulting integrals, a closed-form expression for  $\tilde{P}_2$  can be obtained, as

$$\begin{aligned}\tilde{P}_2 &= 1 - \frac{\gamma\left(m_{sk}, \frac{\tilde{\lambda}_{sk}\phi}{\mathcal{P}\tilde{\lambda}_{sk}^{-v_{sn}}}\right)}{\Gamma(m_{sn})} - \sum_{j=0}^{m_{kd}-1} \frac{\tilde{\lambda}_{kd}^j}{\Gamma(j+1)} \sum_{q=0}^j \binom{j}{q} \left(\frac{\tau \eta_2}{\eta_1}\right)^q \left(\frac{\tau - 1}{\eta_1 \Gamma_t}\right)^{j-q} \frac{\tilde{\lambda}_{sk}^{m_{sk}}}{\Gamma(m_{sk})} \exp\left(-\frac{\tilde{\lambda}_{sk}\phi}{\mathcal{P}d_{sk}'^{-u_{sk}}}\right) \\ &\times \sum_{p=0}^{m_{sk}-1} \binom{m_{sk}-1}{p} \left(\frac{\phi}{\mathcal{P}d_{sk}'^{-u_{sk}}}\right)^{m_{sk}-1-p} 2 \left(\frac{\tilde{\lambda}_{kd}(\tau - 1)}{\tilde{\lambda}_{sk}\eta_1 \Gamma_t}\right)^{\frac{p+q-j+1}{2}} K_{p+q-j+1}\left(\sqrt{\frac{4\tilde{\lambda}_{sk}\tilde{\lambda}_{kd}(\tau - 1)}{\eta_1 \Gamma_t}}\right) \\ &\times \sum_{l=1}^N \binom{N}{l} (-1)^{l+1} \sum_{\substack{n_1, n_2, \dots, n_{m_{ke}} \geq 0 \\ n_1 + n_2 + \dots + n_{m_{ke}} = l}} \delta(l, \theta_3, \theta_4, \tilde{\lambda}_{ke}) \left(\tilde{\lambda}_{ke}\theta_3 + \frac{\tilde{\lambda}_{kd}\tau\eta_2}{\eta_1}\right)^{-(\theta_4+q)} \Gamma(\theta_4 + q + 1) \\ &\times \left(\frac{\tilde{\lambda}_{ke}\theta_3}{\tilde{\lambda}_{ke}\theta_3 + \frac{\tilde{\lambda}_{kd}\tau\eta_2}{\eta_1}} - \frac{\theta_4}{\theta_4 + q}\right).\end{aligned}\quad (28)$$

A detail solution of  $\tilde{P}_2$  for the METS protocol is given in Appendix B. Table I presents the exact SOP for the METS protocol on page 12.

3) *OTS Protocol*: In the OTS method, the tag chosen is the one with the highest instantaneous secrecy capacity. The optimal tag is identified based on the condition

$$k^* = \arg \max_{1 \leq k \leq N} \mathcal{C}_{sec}(\gamma_d^k, \gamma_e^k). \quad (29)$$

Given the independence of all channels, the total SOP for this selection approach is derived as the product of the individual SOPs, ie, [12]

$$\tilde{P}_{out} = (\mathbb{P}(\beta_k^* = 0) + \mathbb{P}(\beta_k^* > 0, \mathcal{C}_{sec}(\gamma_d^k, \gamma_e^k) < \mathcal{R}))^N. \quad (30)$$

Applying similar mathematical steps used for deriving the SOP of the METS protocol, the SOP for the OTS protocol can be obtained as provided in Table I on page 12.

4) *RTS Protocol*: In this selection approach, a tag is chosen at random, represented by the formulation

$$k^* = \arg \max_{1 \leq k \leq N} \mathcal{C}_{sec}(\gamma_d^k, \gamma_e^k). \quad (31)$$

Applying similar mathematical steps used for deriving the SOP of the SOTS protocol, the SOP for the RTS protocol can be obtained as given in Table I on page 12.

### B. Exact IP Analysis

In a BackCom network, the IP represents the probability that the eavesdropper successfully intercepts. Mathematically, the IP of any protocol can generally be written as [12]

$$\tilde{P}_{ip} = \underbrace{\mathbb{P}(\beta_k^* = 0)}_{=\tilde{P}_1} + \underbrace{\mathbb{P}(\beta_k^* > 0, \gamma_d^k < \gamma_e^k)}_{=\tilde{P}_3}. \quad (32)$$

Following a similar mathematical approach as used for the SOP derivation, the IP expressions for each selection method are derived and summarized in Table II on page 13.

### C. Asymptotic Analysis

To explore the key factors influencing SOP and IP more thoroughly, we conduct an asymptotic performance analysis under the assumption of very high transmission power, where  $\Gamma_t$  or  $\mathcal{P}$  approaches infinity.

1) *Asymptotic SOP*: The asymptotic SOP of any protocol can write as

$$\tilde{P}_{out}^\infty = \tilde{P}_1^\infty + \tilde{P}_2^\infty, \quad (33)$$

where

$$\tilde{P}_1^\infty = \lim_{\Gamma_t \rightarrow \infty} \tilde{P}_1 = \lim_{\mathcal{P} \rightarrow \infty} \frac{\gamma \left( m_{sk}, \frac{\tilde{\lambda}_{sk} \phi}{\mathcal{P} d_{sk}^{\alpha_{sk}}} \right)}{\Gamma(m_{sk})} = 0, \quad (34)$$

and

$$\begin{aligned} \tilde{P}_2^\infty &= \lim_{\Gamma_t \rightarrow \infty} \tilde{P}_2 = \lim_{\Gamma_t \text{ or } \mathcal{P} \rightarrow \infty} \mathbb{P} \left( W_1 > 0, W_2 < \frac{\tau \eta_2 w_3}{\eta_1} \right) \\ &= \int_0^\infty \int_0^\infty F_{W_2} \left( \frac{\tau \eta_2 w_3}{\eta_1} \right) f_{W_1}(w_1) f_{W_3}(w_3) dw_1 dw_3. \end{aligned} \quad (35)$$

TABLE I  
EXACT SOP EXPRESSIONS

Protocol	SOP
SOTS	$\tilde{P}_{out} = \frac{\gamma \left( m_{sk}, \frac{\tilde{\lambda}_{sk}\phi}{\mathcal{P}d_{sk}^{\prime -u_{sk}}} \right)}{\Gamma(m_{sk})} + \left( \frac{\tilde{\lambda}_{sk}^{m_{sk}} \tilde{\lambda}_{ke}^{m_{ke}}}{\Gamma(m_{sk})\Gamma(m_{ke})} \right) \sum_{\substack{n_1, n_2, \dots, n_{m_{kd}+1} \geq 0 \\ n_1 + n_2 + \dots + n_{m_{kd}+1} = N}} \delta(N, \theta_1, \theta_2, \tilde{\lambda}_{kd}) \sum_{q=0}^{\theta_2} \binom{\theta_2}{q} \left( \frac{\tau\eta_2}{\eta_1} \right)^q$ $\times \exp \left( -\frac{\tilde{\lambda}_{sk}\phi}{\mathcal{P}d_{sk}^{\prime -u_{sk}}} \right) \left( \frac{\tau-1}{\eta_1\Gamma_t} \right)^{\theta_2 - q} \sum_{p=0}^{m_{sk}-1} \binom{m_{sk}-1}{p} \left( \frac{\phi}{\mathcal{P}d_{sk}^{\prime -u_{sk}}} \right)^{m_{sk}-1-p} 2 \left( \frac{\tilde{\lambda}_{kd}\theta_1(\tau-1)}{\eta_1\Gamma_t\tilde{\lambda}_{sk}} \right)^{\frac{p+q-\theta_2+1}{2}}$ $\times K_{p+q-\theta_2+1} \left( \sqrt{\frac{4\theta_1\tilde{\lambda}_{sk}\tilde{\lambda}_{kd}(\tau-1)}{\eta_1\Gamma_t}} \right) \left( \tilde{\lambda}_{ke} + \frac{\tilde{\lambda}_{kd}\theta_1\tau\eta_2}{\eta_1} \right)^{-m_{ke}-q} \Gamma(m_{ke}+q).$
METS	$\tilde{P}_{out} = 1 - \frac{\gamma \left( m_{sk}, \frac{\tilde{\lambda}_{sk}\phi}{\mathcal{P}\tilde{\lambda}_{sk}^{-v_{sn}}} \right)}{\Gamma(m_{sn})} - \sum_{j=0}^{m_{kd}-1} \frac{\tilde{\lambda}_{kd}^j}{\Gamma(j+1)} \sum_{q=0}^j \binom{j}{q} \left( \frac{\tau\eta_2}{\eta_1} \right)^q \left( \frac{\tau-1}{\eta_1\Gamma_t} \right)^{j-q} \frac{\tilde{\lambda}_{sk}^{m_{sk}}}{\Gamma(m_{sk})} \exp \left( -\frac{\tilde{\lambda}_{sk}\phi}{\mathcal{P}d_{sk}^{\prime -u_{sk}}} \right)$ $\times \sum_{p=0}^{m_{sk}-1} \binom{m_{sk}-1}{p} \left( \frac{\phi}{\mathcal{P}d_{sk}^{\prime -u_{sk}}} \right)^{m_{sk}-1-p} 2 \left( \frac{\tilde{\lambda}_{kd}(\tau-1)}{\tilde{\lambda}_{sk}\eta_1\Gamma_t} \right)^{\frac{p+q-j+1}{2}} K_{p+q-j+1} \left( \sqrt{\frac{4\tilde{\lambda}_{sk}\tilde{\lambda}_{kd}(\tau-1)}{\eta_1\Gamma_t}} \right)$ $\times \sum_{l=1}^N \binom{N}{l} (-1)^{l+1} \sum_{\substack{n_1, n_2, \dots, n_{m_{ke}} \geq 0 \\ n_1 + n_2 + \dots + n_{m_{ke}} = l}} \delta(l, \theta_3, \theta_4, \tilde{\lambda}_{ke}) \left( \tilde{\lambda}_{ke}\theta_3 + \frac{\tilde{\lambda}_{kd}\tau\eta_2}{\eta_1} \right)^{-(\theta_4+q)} \Gamma(\theta_4+q+1)$ $\times \left( \frac{\tilde{\lambda}_{ke}\theta_3}{\tilde{\lambda}_{ke}\theta_3 + \frac{\tilde{\lambda}_{kd}\tau\eta_2}{\eta_1}} - \frac{\theta_4}{\theta_4+q} \right).$
OTS	$\tilde{P}_{out} = \left( 1 - \frac{\tilde{\lambda}_{sk}^{m_{sk}} \tilde{\lambda}_{ke}^{m_{ke}}}{\Gamma(m_{sk})\Gamma(m_{ke})} \sum_{j=0}^{m_{kd}-1} \frac{\tilde{\lambda}_{kd}^j}{\Gamma(j+1)} \sum_{q=0}^j \binom{j}{q} \exp \left( -\frac{\tilde{\lambda}_{sk}\phi}{\mathcal{P}d_{sk}^{\prime -u_{sk}}} \right) \left( \frac{\tau-1}{\eta_1\Gamma_t} \right)^{j-q} \sum_{p=0}^{m_{sk}-1} \binom{m_{sk}-1}{p} \right)$ $\times \left( \frac{\phi}{\mathcal{P}d_{sk}^{\prime -u_{sk}}} \right)^{m_{sk}-1-p} 2 \left( \frac{\tilde{\lambda}_{kd}(\tau-1)}{\tilde{\lambda}_{sk}\eta_1\Gamma_t} \right)^{\frac{p+q-j+1}{2}} K_{p+q-j+1} \left( \sqrt{\frac{4\tilde{\lambda}_{sk}\tilde{\lambda}_{kd}(\tau-1)}{\eta_1\Gamma_t}} \right) \left( \frac{\tau\eta_2}{\eta_1} \right)^q \Gamma(m_{ke}+q)$ $\times \left( \frac{1}{\tilde{\lambda}_{ke} + \frac{\tilde{\lambda}_{kd}\tau\eta_2}{\eta_1}} \right)^{m_{ke}+q}.$
RTS	$\tilde{P}_{out} = 1 - \frac{1}{N} \sum_{n=1}^N \left( \frac{\tilde{\lambda}_{sk}^{m_{sk}} \tilde{\lambda}_{ke}^{m_{ke}}}{\Gamma(m_{sk})\Gamma(m_{ke})} \right) \sum_{j=0}^{m_{kd}-1} \frac{\lambda_{kd}^j}{\Gamma(j+1)} \sum_{q=0}^j \binom{j}{q} \exp \left( -\frac{\tilde{\lambda}_{sk}\phi}{\mathcal{P}d_{sk}^{\prime -u_{sk}}} \right) \left( \frac{\tau-1}{\eta_1\Gamma_t} \right)^{j-q}$ $\times \sum_{p=0}^{m_{sk}-1} \binom{m_{sk}-1}{p} \left( \frac{\phi}{\mathcal{P}d_{sk}^{\prime -u_{sk}}} \right)^{m_{sk}-1-p} 2 \left( \frac{\tilde{\lambda}_{kd}(\tau-1)}{\tilde{\lambda}_{sk}\eta_1\Gamma_t} \right)^{\frac{p+q-j+1}{2}} K_{p+q-j+1} \left( \sqrt{\frac{4\tilde{\lambda}_{sk}\tilde{\lambda}_{kd}(\tau-1)}{\eta_1\Gamma_t}} \right)$ $+ \left( \frac{\tau\eta_2}{\eta_1} \right)^q \left( \frac{1}{\tilde{\lambda}_{ke} + \frac{\tilde{\lambda}_{kd}\tau\eta_2}{\eta_1}} \right)^{m_{ke}+q} \Gamma(m_{ke}+q).$

The asymptotic SOP for each protocol is derived from (35) using similar techniques as the exact SOP. The asymptotic SOP expressions for all protocols are in Table III on page 14.

TABLE II  
INTERCEPT PROBABILITY EXPRESSIONS

Protocol	IP
SOTS	$\tilde{P}_{ip} = \frac{\gamma \left( m_{sk}, \tilde{\lambda}_{sk} \frac{\phi}{\mathcal{P}_{d_{sk}}^{j-u_{sk}}} \right)}{\Gamma(m_{sk})} + \frac{\tilde{\lambda}_{ke}^{m_{ke}} \Gamma \left( m_{sk}, \tilde{\lambda}_{sk} \frac{\phi}{\mathcal{P}_{d_{sk}}^{j-u_{sk}}} \right)}{\Gamma(m_{sk}) \Gamma(m_{ke})} \sum_{\substack{n_1, n_2, \dots, n_{m_{kd}+1} \geq 0 \\ n_1 + n_2 + \dots + n_{m_{kd}+1} = N}} \delta \left( N, \theta_1, \theta_2, \tilde{\lambda}_{kd} \right) \left( \frac{\eta_2}{\eta_1} \right)^{\theta_2}$ $\times \left( \frac{1}{\tilde{\lambda}_{ke} + \frac{\tilde{\lambda}_{kd} \theta_1 \eta_2}{\eta_1}} \right)^{m_{ke} + \theta_2} \Gamma(m_{ke} + \theta_2).$
METS	$\tilde{P}_{ip} = 1 - \sum_{j=0}^{m_{kd}-1} \left( \frac{\tilde{\lambda}_{kd}^j}{\Gamma(j+1)} \right) \sum_{\substack{n_1, n_2, \dots, n_{m_{ke}} \geq 0 \\ n_1 + n_2 + \dots + n_{m_{ke}} = l}} \delta \left( l, \theta_3, \theta_4, \tilde{\lambda}_{ke} \right) \left( \frac{\eta_2}{\eta_1} \right)^j \frac{\Gamma \left( m_{sk}, \tilde{\lambda}_{sk} \frac{\phi}{\mathcal{P}_{d_{sk}}^{j-u_{sk}}} \right)}{\Gamma(m_{sk})}$ $\times \left( \frac{1}{\lambda_{ke} \theta_3 + \frac{\lambda_{kd} \eta_2}{\eta_1}} \right)^{\theta_4 + j} \left( \lambda_{ke} \theta_3 \left( \frac{1}{\lambda_{ke} \theta_3 + \frac{\lambda_{kd} \eta_2}{\eta_1}} \right) \Gamma(\theta_4 + j + 1) - \theta_4 \Gamma(\theta_4 + j) \right).$
OTS	$\tilde{P}_{ip} = \left( 1 - \left( \frac{\tilde{\lambda}_{ke}^{m_{ke}}}{\Gamma(m_{ke})} \right) \frac{\Gamma \left( m_{sk}, \tilde{\lambda}_{sk} \frac{\phi}{\mathcal{P}_{d_{sk}}^{j-u_{sk}}} \right)}{\Gamma(m_{sk})} \sum_{j=0}^{m_{kd}-1} \frac{\tilde{\lambda}_{kd}^j}{\Gamma(j+1)} \left( \frac{\eta_2}{\eta_1} \right)^j \left( \frac{1}{\tilde{\lambda}_{ke} + \frac{\tilde{\lambda}_{kd} \eta_2}{\eta_1}} \right)^{m_{ke} + j} \right)^N$ $\times \Gamma(m_{ke} + j).$
RTS	$\tilde{P}_{ip} = \frac{1}{N} \sum_{n=1}^N \left( 1 - \left( \frac{\tilde{\lambda}_{ke}^{m_{ke}}}{\Gamma(m_{ke})} \right) \frac{\Gamma \left( m_{sk}, \tilde{\lambda}_{sk} \frac{\phi}{\mathcal{P}_{d_{sk}}^{j-u_{sk}}} \right)}{\Gamma(m_{sk})} \sum_{j=0}^{m_{kd}-1} \frac{\tilde{\lambda}_{kd}^j}{\Gamma(j+1)} \left( \frac{\eta_2}{\eta_1} \right)^j \left( \frac{1}{\tilde{\lambda}_{ke} + \frac{\tilde{\lambda}_{kd} \eta_2}{\eta_1}} \right)^{m_{ke} + j} \right)$ $\times \Gamma(m_{ke} + j).$

2) *Asymptotic IP*: The asymptotic IP of any protocol can write as

$$\tilde{P}_{ip}^{\infty} = \tilde{P}_1^{\infty} + \tilde{P}_3^{\infty}, \quad (36)$$

where

$$\begin{aligned} \tilde{P}_3^{\infty} &= \lim_{\Gamma_t \rightarrow \infty} \tilde{P}_3 = \lim_{\Gamma_t \text{ or } \mathcal{P} \rightarrow \infty} \mathbb{P} \left( W_1 > 0, W_2 < \frac{\eta_2 w_3}{\eta_1} \right) \\ &= \int_0^{\infty} \int_0^{\infty} F_{W_2} \left( \frac{\eta_2 w_3}{\eta_1} \right) f_{W_1}(w_1) f_{W_3}(w_3) dw_1 dw_3. \end{aligned} \quad (37)$$

The asymptotic IP for each protocol is derived by solving (37) using similar mathematical techniques as those applied for the exact IP expressions. The derived asymptotic IP formulations for all protocols are presented in Table IV on page 14.

TABLE III  
ASYMPTOTIC SOP EXPRESSIONS

Protocol	Asymptotic SOP
SOTS	$\tilde{P}_{out}^{\infty} = \sum_{\substack{n_1, n_2, \dots, n_{m_{kd}+1} \geq 0 \\ n_1 + n_2 + \dots + n_{m_{kd}+1} = N}} \delta(N, \theta_1, \theta_2, \tilde{\lambda}_{kd}) \left( \frac{\tau\eta_2}{\eta_1} \right)^{\theta_2} \left( \frac{1}{\tilde{\lambda}_{ke} + \frac{\tilde{\lambda}_{kd}\theta_1\tau\eta_2}{\eta_1}} \right)^{m_{ke}+\theta_2} \Gamma(m_{ke} + \theta_2).$
METS	$\tilde{P}_{out}^{\infty} = 1 - \sum_{j=0}^{m_{kd}-1} \left( \frac{\lambda_{kd}^j}{\Gamma(j+1)} \right) \sum_{\substack{n_1, n_2, \dots, n_{m_{ke}} \geq 0 \\ n_1 + n_2 + \dots + n_{m_{ke}} = l}} \delta(l, \theta_3, \theta_4, \tilde{\lambda}_{ke}) \left( \frac{\tau\eta_2}{\eta_1} \right)^j \left( \frac{1}{\lambda_{ke}\theta_3 + \frac{\lambda_{kd}\tau\eta_2}{\eta_1}} \right)^{\theta_4+j} \\ \times \left( \lambda_{ke}\theta_3 \left( \frac{1}{\lambda_{ke}\theta_3 + \frac{\lambda_{kd}\tau\eta_2}{\eta_1}} \right) \Gamma(\theta_4 + j + 1) - \theta_4 \Gamma(\theta_4 + j) \right).$
OTS	$\tilde{P}_{out}^{\infty} = \left( 1 - \left( \frac{\tilde{\lambda}_{ke}^{m_{ke}}}{\Gamma(m_{ke})} \right) \sum_{j=0}^{m_{kd}-1} \frac{\tilde{\lambda}_{kd}^j}{\Gamma(j+1)} \left( \frac{\tau\eta_2}{\eta_1} \right)^j \left( \frac{1}{\tilde{\lambda}_{ke} + \frac{\tilde{\lambda}_{kd}\tau\eta_2}{\eta_1}} \right)^{m_{ke}+j} \Gamma(m_{ke} + j) \right)^N.$
RTS	$\tilde{P}_{out}^{\infty} = \frac{1}{N} \sum_{n=1}^N \left( 1 - \left( \frac{\tilde{\lambda}_{ke}^{m_{ke}}}{\Gamma(m_{ke})} \right) \sum_{j=0}^{m_{kd}-1} \frac{\tilde{\lambda}_{kd}^j}{\Gamma(j+1)} \left( \frac{\tau\eta_2}{\eta_1} \right)^j \left( \frac{1}{\tilde{\lambda}_{ke} + \frac{\tilde{\lambda}_{kd}\tau\eta_2}{\eta_1}} \right)^{m_{ke}+j} \Gamma(m_{ke} + j) \right).$

TABLE IV  
ASYMPTOTIC IP EXPRESSIONS

Protocol	Asymptotic IP
SOTS	$\tilde{P}_{ip}^{\infty} = \sum_{\substack{n_1, n_2, \dots, n_{m_{kd}+1} \geq 0 \\ n_1 + n_2 + \dots + n_{m_{kd}+1} = N}} \delta(N, \theta_1, \theta_2, \tilde{\lambda}_{kd}) \left( \frac{\eta_2}{\eta_1} \right)^{\theta_2} \left( \frac{1}{\tilde{\lambda}_{ke} + \frac{\tilde{\lambda}_{kd}\theta_1\eta_2}{\eta_1}} \right)^{m_{ke}+\theta_2} \Gamma(m_{ke} + \theta_2).$
METS	$\tilde{P}_{ip}^{\infty} = 1 - \sum_{j=0}^{m_{kd}-1} \left( \frac{\lambda_{kd}^j}{\Gamma(j+1)} \right) \sum_{\substack{n_1, n_2, \dots, n_{m_{ke}} \geq 0 \\ n_1 + n_2 + \dots + n_{m_{ke}} = l}} \delta(l, \theta_3, \theta_4, \tilde{\lambda}_{ke}) \left( \frac{\eta_2}{\eta_1} \right)^j \left( \frac{1}{\lambda_{ke}\theta_3 + \frac{\lambda_{kd}\eta_2}{\eta_1}} \right)^{\theta_4+j} \\ \times \left( \lambda_{ke}\theta_3 \left( \frac{1}{\lambda_{ke}\theta_3 + \frac{\lambda_{kd}\eta_2}{\eta_1}} \right) \Gamma(\theta_4 + j + 1) - \theta_4 \Gamma(\theta_4 + j) \right).$
OTS	$\tilde{P}_{ip}^{\infty} = \left( 1 - \left( \frac{\tilde{\lambda}_{ke}^{m_{ke}}}{\Gamma(m_{ke})} \right) \sum_{j=0}^{m_{kd}-1} \frac{\tilde{\lambda}_{kd}^j}{\Gamma(j+1)} \left( \frac{\eta_2}{\eta_1} \right)^j \left( \frac{1}{\tilde{\lambda}_{ke} + \frac{\tilde{\lambda}_{kd}\eta_2}{\eta_1}} \right)^{m_{ke}+j} \Gamma(m_{ke} + j) \right)^N.$
RTS	$\tilde{P}_{ip}^{\infty} = \frac{1}{N} \sum_{n=1}^N \left( 1 - \left( \frac{\tilde{\lambda}_{ke}^{m_{ke}}}{\Gamma(m_{ke})} \right) \sum_{j=0}^{m_{kd}-1} \frac{\tilde{\lambda}_{kd}^j}{\Gamma(j+1)} \left( \frac{\eta_2}{\eta_1} \right)^j \left( \frac{1}{\tilde{\lambda}_{ke} + \frac{\tilde{\lambda}_{kd}\eta_2}{\eta_1}} \right)^{m_{ke}+j} \Gamma(m_{ke} + j) \right).$

#### IV. NUMERICAL AND SIMULATION RESULTS

Here, we analyze the SOP and IP performance of energy-harvesting BackCom systems with tag selection through numerical evaluations. The accuracy of the derived expressions is further confirmed using Monte Carlo simulations. The parameters related to considered BackCom net-

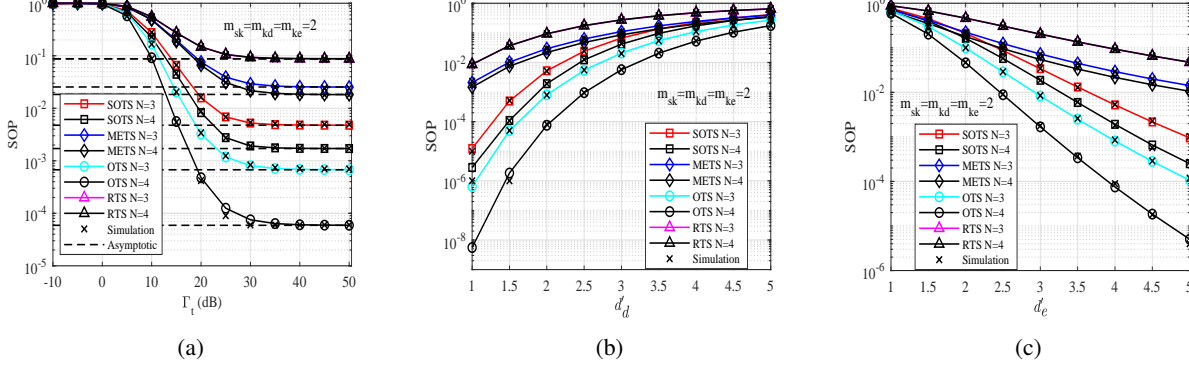


Fig. 2. (a): SOP versus  $\Gamma_t$  for  $N \in \{3, 4\}$ , (b): SOP versus  $d'_d$  for  $N \in \{3, 4\}$ , (c): SOP versus  $d'_e$  for  $N \in \{3, 4\}$ .

work are chosen as:  $P_{max}^{T_k} = 200\mu W$ ,  $\xi_0 = 5\mu W$ ,  $\xi_1 = 5000$ ,  $\xi_2 = 0.0002$  and  $P_c^{T_k} = 200\mu W$ . The channel parameters are set to  $\tilde{\lambda}_{sk} = 2$  dB,  $\tilde{\lambda}_{kd} = 3$  dB and  $\tilde{\lambda}_{ke} = 5$  dB. We assume  $d'_{sk} = d'_s$ , and  $d'_{kx} = d'_x$  for  $k \in \{1, 2, \dots, N\}$ , with a path loss exponent  $u_{sk} = u_{kx} = 2$ ,  $\Gamma_p = 5$  dB, and a tag backscattering coefficient of 2.2. The data rate  $\mathcal{R}$  is measured in bits/s/Hz.

Fig. 2(a) illustrates the SOP as a function of  $\Gamma_t$  for different tag selection schemes with  $N \in \{3, 4\}$ , using the parameters  $d'_s = 1m$ ,  $d'_d = 2m$ ,  $d'_e = 4m$ ,  $\mathcal{R} = 0.5$ , and  $m_{sk} = m_{kd} = m_{ke} = 2$ . The results show that the asymptotic SOP closely matches the analytical results at high SNR, validating the accuracy of the derived expressions. As  $\Gamma_t$  and the number of tags  $N$  increase, the SOP decreases across all schemes, demonstrating that higher transmission power and more selection options improve system secrecy. In terms of performance ranking, the schemes are ordered as OTS, SOTS, METS, and RTS, from best to worst. OTS achieves the lowest SOP because it optimally balances the trade-off between maximizing the desired signal strength and minimizing eavesdropper interference. SOTS follows closely due to its efficient selection based on maximizing power gain while maintaining lower complexity. METS provides moderate performance, as it prioritizes minimizing the strength of the eavesdropper's link but lacks optimality in other aspects. Lastly, RTS shows the highest SOP because it selects tags without considering the channel state information, making it the least effective in ensuring secure communications.

Fig. 2(b) examines the impact of the  $\mathcal{T}_k - D$  distance on the secrecy performance of different tag selection schemes. The analysis uses the parameters  $\Gamma_t = 30$  dB,  $d'_s = 1m$ ,  $d'_e = 4m$ ,  $\mathcal{R} = 0.5$ ,  $m_{sk} = m_{kd} = m_{ke} = 2$ , plotting SOP as a function of distance for varying  $k$  values. The results demonstrate that as the distance between  $\mathcal{T}_k$  and  $D$  increases, the SOP also rises

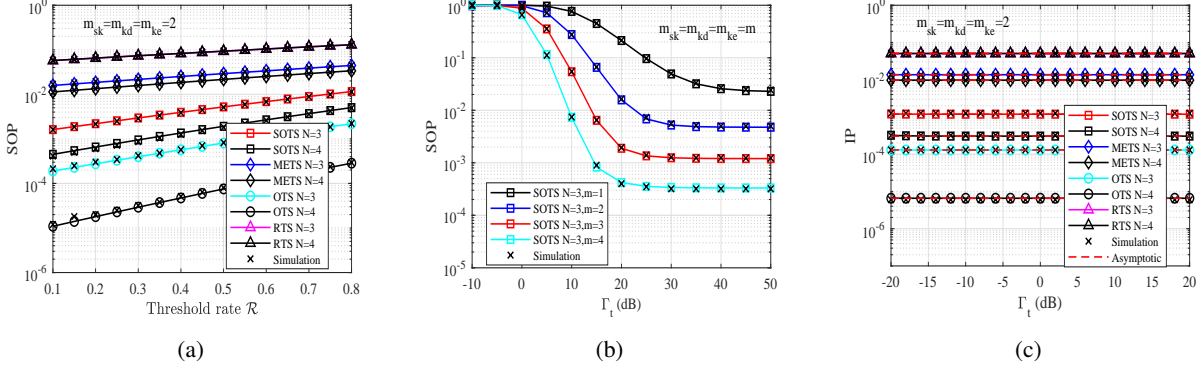


Fig. 3. (a): SOP versus  $\mathcal{R}$  for  $N \in \{3, 4\}$ , (b): SOP versus  $\Gamma_t$  for  $m \in \{1, 2, 3, 4\}$ , (c): IP versus  $\Gamma_t$  for  $N \in \{3, 4\}$ .

due to the greater path loss, which weakens the legitimate communication link relative to the eavesdropper's link. The performance gap between SOTS and METS decreases with larger  $N$ , as more tags improve the chances of selecting one with a favorable  $\mathcal{T}_k - D$  link. OTS remains superior due to its optimal selection strategy, ensuring maximum secrecy capacity regardless of distance. RTS performs the worst, as its random selection ignores channel conditions, making it vulnerable to path loss and eavesdropping. This highlights the critical role of  $\mathcal{T}_k - D$  distance in influencing the effectiveness of tag selection schemes for secure BackCom systems.

Fig. 2(c) illustrates the influence of  $\mathcal{T}_k - E$  distance on secrecy performance, with SOP plotted against  $d'_e$  for various  $N$  and fixed  $m_{sk} = m_{kd} = m_{ke} = 2$ . The results show that SOP improves as the eavesdropper moves farther from the tag, primarily due to increased path loss reducing the eavesdropper's received signal strength. This highlights the significance of spatial placement in enhancing the security of BackCom systems.

Fig. 3(a) shows SOP as a function of the threshold rate  $\mathcal{R}$  for various selection schemes with  $N \in \{3, 4\}$  and  $m_{sk} = m_{kd} = m_{ke} = 2$ . SOP increases with higher threshold rates due to stricter secrecy requirements. The performance improves with more tags, as additional options enhance the likelihood of selecting a tag with favorable channel conditions. Among all schemes, OTS consistently achieves the best performance, with a more pronounced SOP improvement observed for  $N = 4$ , showcasing the effectiveness of optimal tag selection in securing communication under tighter secrecy constraints.

Fig. 3(b) illustrates the SOP as a function of  $\Gamma_t$  for the SOTS scheme with  $N = 3$  and varying fading parameters  $m$  ( $m_{sk} = m_{kd} = m_{ke} = m$ ). The results reveal that as  $m$  increases, the SOP improves due to reduced fading severity. This trend occurs because higher values of  $m$  corre-



spond to less severe channel fluctuations, resulting in more stable and reliable communication links. Consequently, increasing  $m$  enhances the system's secrecy performance by reducing the probability of eavesdropping success.

Fig. 3(c) illustrates IP as a function of  $\Gamma_t$  for various selection schemes with  $N \in \{3, 4\}$  and  $m_{sk} = m_{kd} = m_{ke} = 2$ . Consistent with the trends observed for SOP, IP shows improvement as  $\Gamma_t$  and  $N$  increase, primarily due to the expanded set of available tags, which enhances the chances of selecting one with favorable communication conditions.

## V. CONCLUSION

This paper investigates the secrecy performance of EH BackCom systems using various tag selection schemes-including SOTS, METS, OTS, and RTS-in Nakagami- $m$  fading channels. We derived closed-form expressions for SOP and IP to compare all schemes. We also provided asymptotic expressions for SOTS, METS, OTS, and RTS, offering deeper insights into performance trade-offs. The performance comparison of these selection protocols in terms of SOP is as follows: OTS demonstrates the best performance, followed by SOTS, METS, and finally RTS. Nakagami- $m$  fading proves valuable in analyzing how different channel conditions impact secure communications. Our derived theoretical results verified by simulation results.

## APPENDIX

### A. Derivation of $\tilde{P}_2$ for SOTS

Using binomial expansion and after simplifying, the  $F_{W_2}(\cdot)$  can be written as

$$\begin{aligned}
 F_{W_2} \left( \frac{\tau - 1}{\beta_n^* \eta_1 \Gamma_t w_1} + \frac{\tau \eta_2 w_3}{\eta_1} \right) &= \sum_{\substack{n_1, n_2, \dots, n_{m_{kd}+1} \geq 0 \\ n_1 + n_2 + \dots + n_{m_{kd}+1} = N}} \delta \left( N, \theta_1, \theta_2, \tilde{\lambda}_{kd} \right) \sum_{q=0}^{\theta_2} \binom{\theta_2}{q} \left( \frac{\tau \eta_2}{\eta_1} \right)^q \\
 &\times \left( \frac{\tau - 1}{\eta_1 \Gamma_t \left( w_1 - \frac{\phi}{\mathcal{P}_{d_{sk}}'^{-u_{sk}}} \right)} \right)^{\theta_2 - q} \exp \left( - \frac{(\tau - 1) \tilde{\lambda}_{kd} \theta_1}{\eta_1 \Gamma_t \left( w_1 - \frac{\phi}{\mathcal{P}_{d_{sk}}'^{-u_{sk}}} \right)} \right) w_3^q \exp \left( - \frac{\tilde{\lambda}_{kd} \theta_1 \tau \eta_2 w_3}{\eta_1} \right).
 \end{aligned} \tag{38}$$

By substituting  $F_{W_2}(\cdot)$  which is given in (38) into (19), we can obtain

$$\tilde{P}_2 = \sum_{\substack{n_1, n_2, \dots, n_{m_{kd}+1} \geq 0 \\ n_1 + n_2 + \dots + n_{m_{kd}+1} = N}} \delta \left( N, \theta_1, \theta_2, \tilde{\lambda}_{kd} \right) \sum_{q=0}^{\theta_2} \binom{\theta_2}{q} \left( \frac{\tau \eta_2}{\eta_1} \right)^q \mathcal{I}_1 \mathcal{I}_2, \tag{39}$$

where

$$\mathcal{I}_1 = \int_{\frac{\phi}{\mathcal{P}d'_{sk}-u_{sk}}}^{\infty} \left( \frac{\tau - 1}{\eta_1 \Gamma_t \left( w_1 - \frac{\phi}{\mathcal{P}d'_{sk}-u_{sk}} \right)} \right)^{\theta_2 - q} \exp \left( - \frac{(\tau - 1) \tilde{\lambda}_{kd} \theta_1}{\eta_1 \Gamma_t \left( w_1 - \frac{\phi}{\mathcal{P}d'_{sk}-u_{sk}} \right)} \right) f_{W_1}(w_1) dw_1, \quad (40)$$

and

$$\mathcal{I}_2 = \int_0^{\infty} w_3^q \exp \left( - \frac{\tilde{\lambda}_{kd} \theta_1 \tau \eta_2}{\eta_1} w_3 \right) f_{W_3}(w_3) dw_3. \quad (41)$$

Substituting  $f_{W_1}(\cdot)$  into (40) and applying change of variable  $v_1 = w_1 - \frac{\phi}{\mathcal{P}d'_{sk}-u_{sk}}$ , we can obtain

$$\begin{aligned} \mathcal{I}_1 &= \exp \left( - \frac{\tilde{\lambda}_{sk} \phi}{\mathcal{P}d'_{sk}-u_{sk}} \right) \left( \frac{\tau - 1}{\eta_1 \Gamma_t} \right)^{\theta_2 - q} \int_0^{\infty} v_1^{q - \theta_2} \left( v_1 + \frac{\phi}{\mathcal{P}d'_{sk}-u_{sk}} \right)^{m_{sk} - 1} \\ &\quad \times \exp \left( - \left( \tilde{\lambda}_{sk} v_1 + \frac{(\tau - 1) \tilde{\lambda}_{kd} \theta_1}{\eta_1 \Gamma_t v_1} \right) \right) dv_1. \end{aligned} \quad (42)$$

Furthermore, using binomial expansion for  $\left( v_1 + \frac{\phi}{\mathcal{P}d'_{sk}-u_{sk}} \right)^{m_{sk} - 1}$ , we can get

$$\begin{aligned} \mathcal{I}_1 &= \exp \left( - \frac{\tilde{\lambda}_{sk} \phi}{\mathcal{P}d'_{sk}-u_{sk}} \right) \left( \frac{\tau - 1}{\eta_1 \Gamma_t} \right)^{\theta_2 - q} \sum_{p=0}^{m_{sk} - 1} \binom{m_{sk} - 1}{p} \left( \frac{\phi}{\mathcal{P}d'_{sk}-u_{sk}} \right)^{m_{sk} - 1 - p} \\ &\quad \times \int_0^{\infty} v_1^{p + q - \theta_2} \exp \left( - \left( \tilde{\lambda}_{sk} v_1 + \frac{(\tau - 1) \tilde{\lambda}_{kd} \theta_1}{\eta_1 \Gamma_t v_1} \right) \right) dv_1. \end{aligned} \quad (43)$$

Using [19, (2.3.16.1)], we can get a closed-form solution of  $\mathcal{I}_1$  as

$$\begin{aligned} \mathcal{I}_1 &= \exp \left( - \frac{\tilde{\lambda}_{sk} \phi}{\mathcal{P}d'_{sk}-u_{sk}} \right) \left( \frac{\tau - 1}{\eta_1 \Gamma_t} \right)^{\theta_2 - q} \sum_{p=0}^{m_{sk} - 1} \binom{m_{sk} - 1}{p} \left( \frac{\phi}{\mathcal{P}d'_{sk}-u_{sk}} \right)^{m_{sk} - 1 - p} \\ &\quad \times \left( 2 \left( \frac{\tilde{\lambda}_{kd} \theta_1 (\tau - 1)}{\eta_1 \Gamma_t \tilde{\lambda}_{sk}} \right)^{\frac{p + q - \theta_2 + 1}{2}} K_{p + q - \theta_2 + 1} \left( \sqrt{\frac{4 \theta_1 \tilde{\lambda}_{sk} \tilde{\lambda}_{kd} (\tau - 1)}{\eta_1 \Gamma_t}} \right) \right). \end{aligned} \quad (44)$$

Substituting  $f_{W_3}(\cdot)$  into (41) and solving the integral using [15, (8.310.1)], we can obtain a closed-form solution of  $\mathcal{I}_2$  as

$$\mathcal{I}_2 = \left( \tilde{\lambda}_{ke} + \frac{\tilde{\lambda}_{kd} \theta_1 \tau \eta_2}{\eta_1} \right)^{-m_{ke} - q} \Gamma(m_{ke} + q). \quad (45)$$

Using (44) and (45) into (39), we can get a new closed-form expression of  $\tilde{P}_2$  which is given in (20) on page 8.

### B. Derivation of $\tilde{P}_2$ for METS

By substituting  $F_{W_2}(\cdot)$  which is given in (4) into (27), we can obtain

$$\tilde{P}_2 = \mathcal{I}_3 - \sum_{j=0}^{m_{ke}-1} \frac{\tilde{\lambda}_{kd}^j}{\Gamma(j+1)} \mathcal{I}_4, \quad (46)$$

where

$$\mathcal{I}_3 = \int_0^\infty \int_{\frac{\phi}{\mathcal{P}_{sk}^{d'-u_{sk}}}}^\infty f_{W_1}(w_1) f_{W_3}(w_3) dw_1 dw_3, \quad (47)$$

and

$$\begin{aligned} \mathcal{I}_4 &= \int_0^\infty \int_{\frac{\phi}{\mathcal{P}_{sk}^{d'-u_{sk}}}}^\infty \left( \frac{\tau-1}{\eta_1 \Gamma_t \beta_k^* w_1} + \frac{w_3}{\eta_1} \right)^j \exp \left( -\tilde{\lambda}_{kd} \left( \frac{\tau-1}{\eta_1 \Gamma_t \beta_k^* w_1} + \frac{w_3}{\eta_1} \right) \right) \\ &\quad \times f_{W_1}(w_1) f_{W_3}(w_3) dw_1 dw_3. \end{aligned} \quad (48)$$

Using properties of PDF and CDF, we can obtain a closed-form solution of  $\mathcal{I}_3$  as

$$\mathcal{I}_3 = \int_0^\infty f_{W_3}(w_3) dw_3 \int_{\frac{\phi}{\mathcal{P}_{sk}^{d'-u_{sk}}}}^\infty f_{W_1}(w_1) dw_1 = 1 - \frac{\gamma \left( m_{sk}, \frac{\tilde{\lambda}_{sk} \phi}{\mathcal{P}_{sk}^{d'-u_{sk}}} \right)}{\Gamma(m_{sk})}. \quad (49)$$

Using binomial expansion for  $\left( \frac{\tau-1}{\eta_1 \Gamma_t \beta_k^* w_1} + \frac{w_3}{\eta_1} \right)^j$  and simplification, we can write

$$\mathcal{I}_4 = \sum_{q=0}^j \binom{j}{q} \left( \frac{\tau \eta_2}{\eta_1} \right)^q \mathcal{I}_{41} \mathcal{I}_{42}, \quad (50)$$

where

$$\mathcal{I}_{41} = \int_{\frac{\phi}{\mathcal{P}_{sk}^{d'-u_{sk}}}}^\infty \left( \frac{\tau-1}{\eta_1 \Gamma_t \left( w_1 - \frac{\phi}{\mathcal{P}_{sk}^{d'-u_{sk}}} \right)} \right)^{j-q} \exp \left( -\frac{(\tau-1) \tilde{\lambda}_{kd}}{\eta_1 \Gamma_t \left( w_1 - \frac{\phi}{\mathcal{P}_{sk}^{d'-u_{sk}}} \right)} \right) f_{W_1}(w_1) dw_1, \quad (51)$$

and

$$\mathcal{I}_{42} = \int_0^\infty w_3^q \exp\left(-\frac{\tilde{\lambda}_{kd}\theta_1\tau\eta_2}{\eta_1}w_3\right) f_{W_3}(w_3) dw_3. \quad (52)$$

Substituting  $f_{W_1}(\cdot)$  into (51) and applying change of variable  $v_1 = w_1 - \frac{\phi}{\mathcal{P}d_{sk}'^{-u_{sk}}}$ , we can obtain as

$$\begin{aligned} \mathcal{I}_{41} &= \left(\frac{\tau-1}{\eta_1\Gamma_t}\right)^{j-q} \frac{(\tilde{\lambda}_{sk}^{m_{sk}})}{\Gamma(m_{sk})} \exp\left(-\frac{\tilde{\lambda}_{sk}\phi}{\mathcal{P}d_{sk}'^{-u_{sk}}}\right) \int_0^\infty v_1^{q-j} \left(v_1 + \frac{\phi}{\mathcal{P}d_{sk}'^{-u_{sk}}}\right)^{m_{sk}-1} \\ &\quad \times \exp\left(-\left(\tilde{\lambda}_{sk}v_1 + \frac{(\tau-1)\tilde{\lambda}_{kd}}{\eta_1\Gamma_tv_1}\right)\right) dv_1. \end{aligned} \quad (53)$$

Using binomial expansion for  $\left(v_1 + \frac{\phi}{\mathcal{P}d_{sk}'^{-u_{sk}}}\right)^{m_{sk}-1}$  in (53), we can get as

$$\begin{aligned} \mathcal{I}_{41} &= \left(\frac{\tau-1}{\eta_1\Gamma_t}\right)^{j-q} \frac{(\tilde{\lambda}_{sk}^{m_{sk}})}{\Gamma(m_{sk})} \exp\left(-\frac{\tilde{\lambda}_{sk}\phi}{\mathcal{P}d_{sk}'^{-u_{sk}}}\right) \sum_{p=0}^{m_{sk}-1} \binom{m_{sk}-1}{p} \left(\frac{\phi}{\mathcal{P}d_{sk}'^{-u_{sk}}}\right)^{m_{sk}-1-p} \int_0^\infty v_1^{p+q-k} \\ &\quad \times \exp\left(-\left(\tilde{\lambda}_{sk}v_1 + \frac{(\tau-1)\tilde{\lambda}_{kd}}{\eta_1\Gamma_tv_1}\right)\right) dv_1. \end{aligned} \quad (54)$$

Using [19, (2.3.16.1)], we can get a closed-form solution of  $\mathcal{I}_{41}$  as

$$\begin{aligned} \mathcal{I}_{41} &= \left(\frac{\tau-1}{\eta_1\Gamma_t}\right)^{j-q} \frac{(\tilde{\lambda}_{sk}^{m_{sk}})}{\Gamma(m_{sk})} \exp\left(-\frac{\tilde{\lambda}_{sk}\phi}{\mathcal{P}d_{sk}'^{-u_{sk}}}\right) \sum_{p=0}^{m_{sk}-1} \binom{m_{sk}-1}{p} \left(\frac{\phi}{\mathcal{P}d_{sk}'^{-u_{sk}}}\right)^{m_{sk}-1-p} \\ &\quad \times \left(2 \left(\frac{\tilde{\lambda}_{kd}(\tau-1)}{\eta_1\Gamma_t\tilde{\lambda}_{sk}}\right)^{\frac{p+q-j+1}{2}} K_{p+q-j+1}\left(\sqrt{\frac{4\tilde{\lambda}_{sk}\tilde{\lambda}_{kd}(\tau-1)}{\eta_1\Gamma_t}}\right)\right). \end{aligned} \quad (55)$$

Substituting  $f_{W_3}(\cdot)$  into (52) and solving the integral using [15, (8.310.1)], we can obtain a closed-form solution of  $\mathcal{I}_{42}$  as

$$\begin{aligned} \mathcal{I}_{42} &= \sum_{l=1}^N \binom{N}{l} (-1)^{l+1} \sum_{\substack{n_1, n_2, \dots, n_{m_{ke}} \geq 0 \\ n_1 + n_2 + \dots + n_{m_{ke}} = l}} \delta(l, \theta_3, \theta_4, \tilde{\lambda}_{ke}) \left(\tilde{\lambda}_{ke}\theta_3 + \frac{\tilde{\lambda}_{kd}\tau\eta_2}{\eta_1}\right)^{-(\theta_4+q)} \Gamma(\theta_4+q+1) \\ &\quad \times \left(\frac{\tilde{\lambda}_{ke}\theta_3}{\tilde{\lambda}_{ke}\theta_3 + \frac{\tilde{\lambda}_{kd}\tau\eta_2}{\eta_1}} - \frac{\theta_4}{\theta_4+q}\right). \end{aligned} \quad (56)$$

Using (49) and (50) into (46), we can get a new closed-form expression of  $\tilde{P}_2$  which is given in (28) on page 10.

## REFERENCES

- [1] A. Kludze, J. Kono, D. M. Mittleman, and Y. Ghasempour, "A frequency-agile retrodirective tag for large-scale sub-terahertz data backscattering," *Nature Communications*, vol. 15, no. 1, p. 8756, 2024.
- [2] N. Van Huynh, D. T. Hoang, X. Lu, D. Niyato, P. Wang, and D. I. Kim, "Ambient backscatter communications: A contemporary survey," *IEEE Communications surveys & tutorials*, vol. 20, no. 4, pp. 2889–2922, 2018.
- [3] S. Jia, R. Wang, Y. Xu, Y. Lou, D. Zhang, and T. Sato, "Secrecy analysis of abcom-based intelligent transportation systems with jamming," *IEEE Transactions on Intelligent Transportation Systems*, vol. 25, no. 3, pp. 2880–2892, 2024.
- [4] E. Illi, M. Qaraqe, S. Althunibat, A. Alhasanat, M. Alsafasfeh, M. de Ree, G. Mantas, J. Rodriguez, W. Aman, and S. Al-Kuwari, "Physical layer security for authentication, confidentiality, and malicious node detection: a paradigm shift in securing IoT networks," *IEEE Communications Surveys & Tutorials*, vol. 26, no. 1, pp. 347–388, 2023.
- [5] J. M. Hamamreh, H. M. Furqan, and H. Arslan, "Classifications and applications of physical layer security techniques for confidentiality: A comprehensive survey," *IEEE Communications Surveys & Tutorials*, vol. 21, no. 2, pp. 1773–1828, 2018.
- [6] Y. Liu, Y. Ye, and R. Q. Hu, "Secrecy outage probability in backscatter communication systems with tag selection," *IEEE Wireless Communications Letters*, vol. 10, no. 10, pp. 2190–2194, 2021.
- [7] W. Saad, X. Zhou, Z. Han, and H. V. Poor, "On the physical layer security of backscatter wireless systems," *IEEE Transactions on Wireless Communications*, vol. 13, no. 6, pp. 3442–3451, 2014.
- [8] Y. Zhang, F. Gao, L. Fan, X. Lei, and G. K. Karagiannidis, "Secure communications for multi-tag backscatter systems," *IEEE Wireless Communications Letters*, vol. 8, no. 4, pp. 1146–1149, 2019.
- [9] Z. Liu, Y. Ye, X. Chu, and H. Sun, "Secrecy performance of backscatter communications with multiple self-powered tags," *IEEE Communications Letters*, vol. 26, no. 12, pp. 2875–2879, 2022.
- [10] T. S. Muratkar, A. Bhurane, P. K. Sharma, and A. Kothari, "Physical layer security analysis in ambient backscatter communication with node mobility and imperfect channel estimation," *IEEE Communications Letters*, vol. 26, no. 1, pp. 27–30, 2022.
- [11] S. Wang, M. Xia, K. Huang, and Y.-C. Wu, "Wirelessly powered two-way communication with nonlinear energy harvesting model: Rate regions under fixed and mobile relay," *IEEE Transactions on Wireless Communications*, vol. 16, no. 12, pp. 8190–8204, 2017.
- [12] Y. Khan, A. Afzal, A. Dubey, and A. Saxena, "Secrecy performance of energy-harvesting backscatter communication network under different tag selection schemes," *IEEE Journal of Radio Frequency Identification*, vol. 8, pp. 43–48, 2024.
- [13] M. K. Simon and M.-S. Alouini, *Digital Communication over Fading Channels*, 2nd ed. New York, NY, USA: Wiley, 2005.
- [14] D. Dixit and P. R. Sahu, "Performance analysis of rectangular QAM with SC receiver over Nakagami- $m$  fading channels," *IEEE Communications Letters*, vol. 18, no. 7, pp. 1262–1265, 2014.
- [15] I. Gradshteyn and I. Ryzhik, *Table of integrals, series, and products*, 7th ed. Elsevier, 2007.
- [16] G. Wang, F. Gao, R. Fan, and C. Tellambura, "Ambient backscatter communication systems: Detection and performance analysis," *IEEE Transactions on Communications*, vol. 64, no. 11, pp. 4836–4846, 2016.
- [17] Y. Ye, L. Shi, X. Chu, and G. Lu, "On the outage performance of ambient backscatter communications," *IEEE Internet of Things Journal*, vol. 7, no. 8, pp. 7265–7278, 2020.
- [18] M. Abramowitz and I. A. Stegun, *Handbook of mathematical functions with formulas, graphs, and mathematical tables*. US Government printing office, 1968, vol. 55.
- [19] A. Prudnikov, Y. A. Brychkov, and O. Marichev, *Integrals and Series: Volume 1*. CRC Press: Boca Rato, FL, USA, 1986.

This figure "Picture1.png" is available in "png" format from:

<http://arxiv.org/ps/2503.12400v1>

